

Numerical Simulation of Fluid Flow on The Transportation of Tourism Ship-Type Catamaran

A H Yunianto^{1*}, R D Putra¹, D Nusyirwan¹, A M Raharja¹

¹Department of Naval Architecture, Faculty of Engineering, Raja Ali Haji Maritime University, Tanjungpinang 29411, Indonesia
{a.hekso@umrah.ac.id¹, risandi@umrah.ac.id¹, denyusyirwan@umrah.ac.id¹}

Abstract. The hull of a ship is the most notable structural entity, which is the watertight enclosure that protects the cargo, machinery, and accommodation spaces of the ship from the weather, flooding, and structural damage. Subsequently, the hull design is essential to other parts to predict the magnitude of the resistance, and each shape of the catamaran affects the fluid flow characteristics. There are currently many catamaran designs found with varying configurations and dimensions. The operational and mission functions heavily influence the design attributes and numerical fluid flow simulation on a catamaran was performed using the Navier-Stokes equation. Subsequently, by solving numerically and simulations, the magnitude of the resistance component acting on the catamaran hull will be known for laminar and turbulent flow. From the simulation results, it is clear that symmetrical and asymmetrical fluid flow around the keel is caused by the emergence of flow interactions between the gutwaves, and the amount of pressure that arises around the keel is asymmetrical relative to the centerline.

Keywords: Numeric, catamaran, navier stokes,

1 Introduction

Currently, catamaran as a form of river and sea transportation is still developing quickly [1]. Several areas of Indonesia currently make extensive use of catamaran as a form of transportation. Furthermore, a vast deck area and a level of stability that is more pleasant and safe are two features that contribute to this ship's high demand [2-3]. In addition, catamaran ship tends to have low water drafts, and they can operate in shallow water, and then the slender hull shape can minimize the occurrence of wave wash.

Catamaran poses many technical challenges in the engineering process compared to conventional ship designs, and this ship is characterized by a more complex configuration and operated at higher speeds. When designing a catamaran, a designer uses experimental techniques (model test) and numerical modeling, and there is a need for more investigation into the challenges and the resistance problem. This is because the resistance component is more complex than a single hull vessel, namely the complexity of the interaction effects of viscous and wave resistance components on the catamarans hull. The interaction of various barrier components is a phenomenon that is still under scientific investigation. Doctor et al. (2003) determined the optimal separation between hulls and predict wave interference. Several studies on gastric spacing have been systematically reviewed by Insel et al. (1991) and Molland et al (1992) [4-6]. It was concluded that changing the distance between the two catamaran hulls had a significant interference effect on the viscous resistance. In addition, wave interference can also affect the wave speed due to changes in the distance between the catamaran hulls.

Many researchers have presented and published the problem of drag in monohull ships. However, for catamarans, the issue of resistance is widely discussed and discussed in scientific forums because the resistance components are more complex than monohull ships due to the interaction and interference effects of the dense and wave resistance components on the catamaran hull. The interaction and interference of the barrier components is still a scientific discussion that continues to develop, especially in enriching and strengthening databases for scientific purposes.

A ship moving in water at a certain speed will experience a drag force (resistance) opposite the direction of the ship's motion. The magnitude of the ship's resistance is greatly influenced by the speed of the boat (V_s), the weight of the water displaced by the hull immersed in water (displacement), and the shape of the hull (hull form).

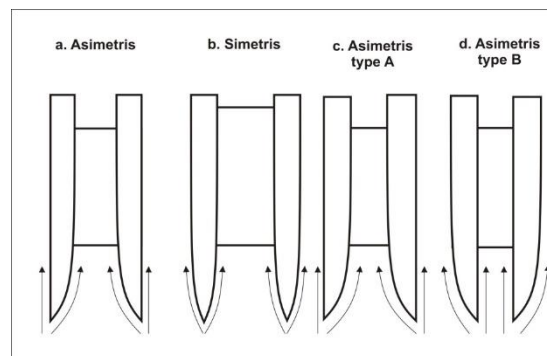


Fig 1. Type of catamaran hull

This study describes the fluid flow scheme around the catamaran hull, the discretization of the Navier-Stokes equation in the form of a differential equation using the finite difference method, forming a system of linear equations, solving a system of linear equations, numerical solutions, and simulations.

2 Research Method

This study described the numerical simulation of the effect of fluid flow acting on a catamaran-like ship. The steps performed were the determination of the continuity equation and momentum from the related cases in question, fluid Mechanics, viscous resistance, wave resistance, finite difference method, and the Navier-Stokes equation. Next is the implementation of the previously created algorithm into the form of a program. With the implemented program, a simulation was carried out using several values in the parameters or input variables.

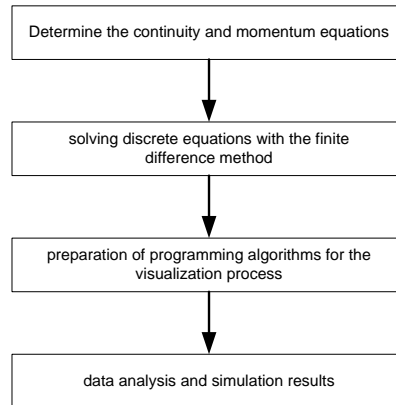


Fig 2. solution flowchart

3. Results and Discussion

3.1 Schematic of fluid flow around the hull of the catamaran

In order to solve the liquid flow problem around the catamaran hull, a diagram is created. Therefore, it can be helpful to describe the problem. The following is a scheme made to represent the problems to be solved (Fig 3).

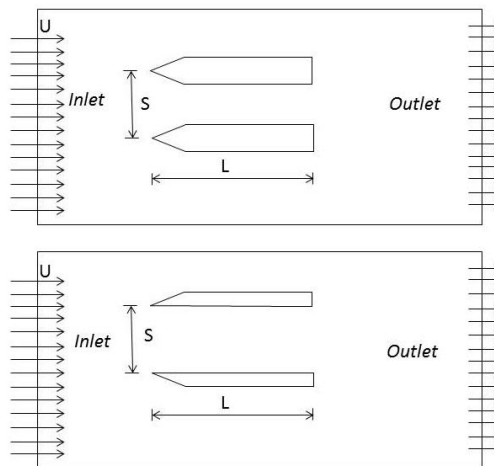


Fig 3 symmetrical catamaran hull configuration model and not symmetrical

Fig 3 explains that a rectangular-shaped domain is used to overlay the distance configuration across (S/L). Where S is the configuration of the transverse distance between the hulls and L is the ship's length in hull configuration. The left arrow indicates that the inlet from the front of the hull is at velocity U, which is parallel to the x-axis. In addition, there is a velocity V parallel to the y-axis.

3.2 Numerical Solution

Derivation of the Navier-Stokes equation for incompressible two-dimensional turbulent flow in two dimensions. The equation of motion and continuity for Newtonian fluids is the Navier-Stokes equation using the finite difference method. Furthermore, the steps to solve the Navier-Stokes equation are presented below: The Navier-Stokes equation for incompressible for unsteady and viscous fluids is given below.

$$\frac{\partial \mathbf{u}}{\partial t} + \nabla \cdot \mathbf{u}\mathbf{u} + \nabla P = \frac{1}{\text{Re}} \nabla^2 \mathbf{u} \quad (1)$$

$$\nabla \cdot \mathbf{u} = 0 \quad (2)$$

With :

\mathbf{u} is the velocity vector in the form (x,y)

P is pressure

Re is Reynolds's number

To solve the Navier-Stokes equation with a numerical scheme, the equation is rewritten into a differential equation.

Momentum Equation

Momentum-x

$$\frac{\partial u}{\partial t} + \frac{\partial uu}{\partial x} + \frac{\partial uv}{\partial y} + \frac{\partial P}{\partial x} = \frac{1}{\text{Re}} \left[\frac{\partial^2 u}{\partial x^2} + \frac{\partial^2 u}{\partial y^2} \right] \quad (3)$$

Momentum-y

$$\frac{\partial v}{\partial t} + \frac{\partial uv}{\partial x} + \frac{\partial vv}{\partial y} + \frac{\partial P}{\partial y} = \frac{1}{\text{Re}} \left[\frac{\partial^2 v}{\partial x^2} + \frac{\partial^2 v}{\partial y^2} \right] \quad (4)$$

1. Continuity Equation

$$\frac{\partial u}{\partial x} + \frac{\partial v}{\partial y} = 0 \quad (5)$$

Then the differential equation is solved by following the flow of the algorithm.

The following are the completion steps using an algorithm.

1. Initial for each component

The initial conditions for the velocity and pressure components are given. There are two velocity components, namely the u -speed component, parallel to the x -axis, and the v -speed component, similar to the y -axis. The sum of the two-speed parts is equal to one with the following details: Then the differential equation is solved by following the flow of the algorithm.

The following are the completion steps using an algorithm.

$$(u^*)^n = 1$$

$$(v^*)^n = 0 \quad (6)$$

2. Computes the value $(u^*)^{n+1}, (v^*)^{n+1}$ ignoring the value $(p^*)^n$ Using the momentum equation to obtain the $(u^*)^{n+1}, (v^*)^{n+1}$ where is the momentum-x equation for solving $(u^*)^{n+1}$ and the momentum equation -y for completion $(v^*)^{n+1}$

The following is a detailed explanation of the calculation of the momentum x and y equation:

$$\frac{\partial u}{\partial t} = -u \frac{\partial u}{\partial x} - v \frac{\partial u}{\partial y} + \frac{1}{\text{Re}} \left[\frac{\partial^2 u}{\partial x^2} + \frac{\partial^2 u}{\partial y^2} \right] \quad (7)$$

$$\frac{\partial v}{\partial t} = -u \frac{\partial v}{\partial x} - v \frac{\partial v}{\partial y} + \frac{1}{\text{Re}} \left[\frac{\partial^2 v}{\partial x^2} + \frac{\partial^2 v}{\partial y^2} \right] \quad (8)$$

Next, substitute the finite differential derivative into the differential equation above to get a system of linear equations.

$$u_{i,j}^{n+1} = u_{i,j}^n + \Delta t \left\{ -u_{i,j}^n \left(\frac{u_{i+1,j}^n - u_{i-1,j}^n}{2\Delta x} \right) - v_{i,j}^n \left(\frac{u_{i,j+1}^n - u_{i,j-1}^n}{2\Delta y} \right) + \frac{1}{\text{Re}} \left[\left(\frac{u_{i+1,j}^n - 2u_{i,j}^n + u_{i-1,j}^n}{(\Delta x)^2} \right) + \left(\frac{u_{i,j+1}^n - 2u_{i,j}^n + u_{i,j-1}^n}{(\Delta y)^2} \right) \right] \right\} \quad (9)$$

$$v_{i,j}^{n+1} = v_{i,j}^n + \Delta t \left\{ -u_{i,j}^n \left(\frac{v_{i+1,j}^n - v_{i-1,j}^n}{2\Delta x} \right) - v_{i,j}^n \left(\frac{v_{i,j+1}^n - v_{i,j-1}^n}{2\Delta y} \right) + \frac{1}{\text{Re}} \left[\left(\frac{v_{i+1,j}^n - 2v_{i,j}^n + v_{i-1,j}^n}{(\Delta x)^2} \right) + \left(\frac{v_{i,j+1}^n - 2v_{i,j}^n + v_{i,j-1}^n}{(\Delta y)^2} \right) \right] \right\} \quad (10)$$

3. Solving temporary stresses using Poisson's equation. After gaining temporary speed ie

$$(u^*)_{i,j}^{n+1} = U = u_{i,j}^n + \Delta t \left\{ -u_{i,j}^n \left(\frac{u_{i+1,j}^n - u_{i-1,j}^n}{2\Delta x} \right) - v_{i,j}^n \left(\frac{u_{i,j+1}^n - u_{i,j-1}^n}{2\Delta y} \right) + \frac{1}{\text{Re}} \left[\left(\frac{u_{i+1,j}^n - 2u_{i,j}^n + u_{i-1,j}^n}{(\Delta x)^2} \right) + \left(\frac{u_{i,j+1}^n - 2u_{i,j}^n + u_{i,j-1}^n}{(\Delta y)^2} \right) \right] \right\} \quad (11)$$

$$(v^*)_{i,j}^{n+1} = V = v_{i,j}^n + \Delta t \left\{ -u_{i,j}^n \left(\frac{v_{i+1,j}^n - v_{i-1,j}^n}{2\Delta x} \right) - v_{i,j}^n \left(\frac{v_{i,j+1}^n - v_{i,j-1}^n}{2\Delta y} \right) + \frac{1}{\text{Re}} \left[\left(\frac{v_{i+1,j}^n - 2v_{i,j}^n + v_{i-1,j}^n}{(\Delta x)^2} \right) + \left(\frac{v_{i,j+1}^n - 2v_{i,j}^n + v_{i,j-1}^n}{(\Delta y)^2} \right) \right] \right\} \quad (12)$$

3.3 Pressure around the hull

The pressure between the hulls of the catamaran with variations in the distance of the hulls can be seen in Figure 2. The pressure between the hulls affects the distance between the hulls (S/L), where the pressure increases as the distance between the hulls (S/L) decreases. The greater the speed of the ship, the greater the pressure that occurs around the hull which is measured by

several pressures with the position on the draft along the hull to determine the distribution of pressure around (between) the hull.

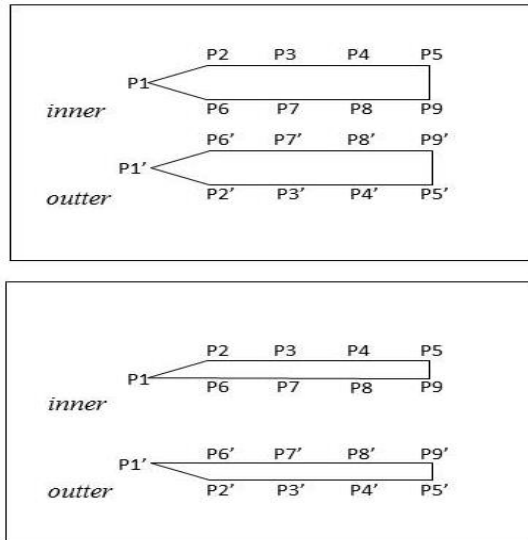


Figure 4. Configuration of pressure measurement positions on symmetrical and asymmetrical catamaran hulls

Table 1. shows the pressure symmetrical catamaran between the hull (inner) P6, P7, P8, P9, P6', P7', P8', P9' greater than outside the hull (outer) P2, P3, P4, P5, P2', P3', P4', P5' and the pressure between the hulls (inner) decreases as the ratio of the distance between the hulls increases from $S/L = 0.2$ to $S/L = 0.4$.

Table 1 Pressure values on symmetrical hull catamarans

Table 1. Pressure values on symmetrical hull catamarans

<i>Position</i>	<i>S/L 0.2</i>	<i>S/L 0.3</i>	<i>S/L 0.4</i>
<i>P1</i>	2010.68	2596.02	2390.87
<i>P2</i>	278.32	351.05	299.72
<i>P3</i>	294.51	533.38	575.88
<i>P4</i>	923.77	938.18	931.71
<i>P5</i>	-440.17	-454.82	223.69
<i>P6</i>	522.85	477.90	353.60
<i>P7</i>	365.45	400.50	541.79

<i>P8</i>	1603.95	1408.29	825.55
<i>P9</i>	261.49	-362.08	323.74
<i>P1'</i>	2006.66	4323.29	2285.36
<i>P2'</i>	273.40	355.16	306.24
<i>P3'</i>	278.83	307.095	553.42
<i>P4'</i>	932.13	935.77	974.21
<i>P5'</i>	-451.97	-366.34	198.65
<i>P6'</i>	507.85	472.39	365.38
<i>P7'</i>	269.97	344.84	542.09
<i>P8'</i>	1608.84	1413.88	839.92
<i>P9'</i>	253.22	-362.08	282.70

Table 2 shows the asymmetrical pressure between the hull (inner) P6, P7, P8, P9, P6', P7', P8', P9' smaller than outside the hull (outer) P2, P3, P4, P5, P2 ',P3',P4',P5' and the pressure between the hulls (inner) decreases as the ratio of the distance between the hulls increases from $S/L = 0.2$ to $S/L = 0.4$

Table 2 Pressure values on asymmetrical hull catamarans

position	S/L 0.2	S/L 0.3	S/L 0.4
P1	1119.28	1760.02	1741.52
P2	507.80	416.13	489.19
P3	479.07	535.52	620.33
P4	761.39	794.09	811.65
P5	-424.92	-237.99	-351.77
P6	806.78	776.03	768.36
P7	620.20	483.15	472.27
P8	691.16	787.04	826.35
P9	-169.04	-203.28	-508.68
P1'	1256.96	1884.84	1447.62
P2'	518.62	430.08	465.35
P3'	452.21	320.29	631.46
P4'	709.42	840.20	631.46
P5'	-416.47	-182.59	-371.05
P6'	807.88	776.03	772.38
P7'	616.16	498.99	531.83
P8'	695.12	770.95	819.91
P9'	-169.04	-240.51	-363.70

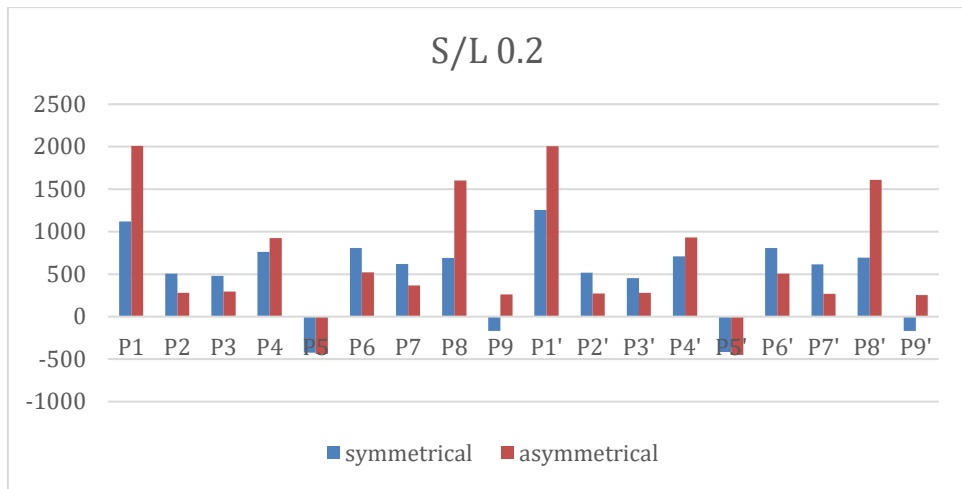


Figure 5. Symmetrical and asymmetrical hull graph with S/L 0.2

Figure 5 shows the pressure between the hulls (inner) on an asymmetrical ship is smaller than that of a symmetrical hull with a distance ratio of S/L 0.2. in the P9 and p9' positions, the asymmetrical stomach did not experience a decrease in pressure compared to the symmetrical stomach.

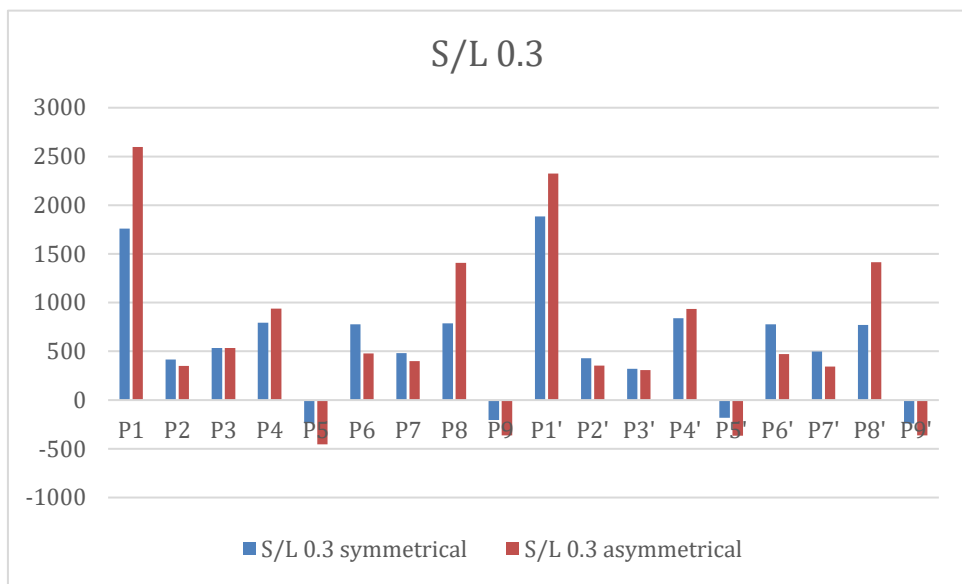


Figure 6. Symmetrical and asymmetrical hull graph with S/L 0.3

Figure 6 shows the pressure between the hulls (inner) on an asymmetrical ship is smaller than that of a symmetrical hull with a distance ratio of S/L 0.3. In the P5, p5', P9, and P9' positions, the symmetrical and asymmetrical stomachs did not experience a decrease in pressure. However, for the asymmetrical stomach, the pressure was smaller than that of the symmetrical stomach.

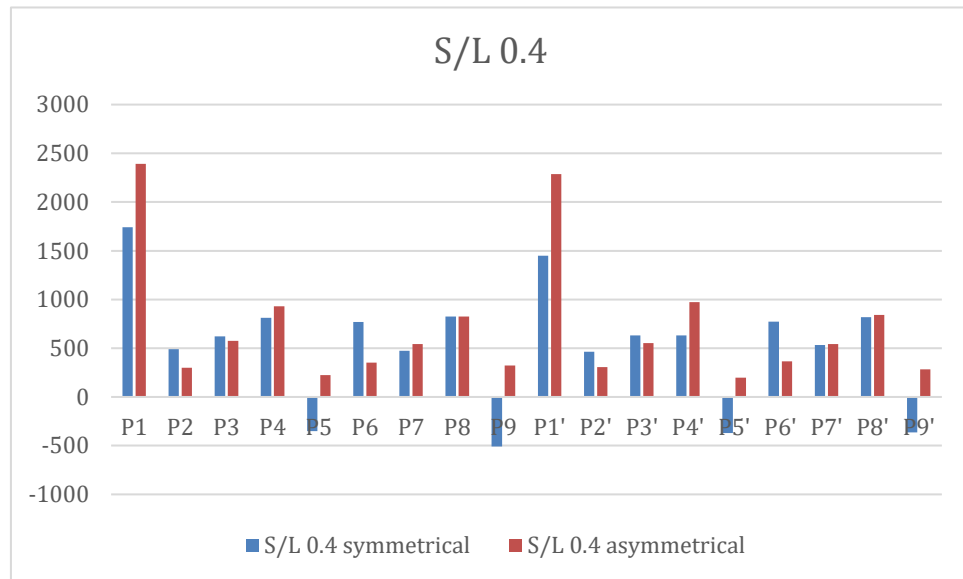
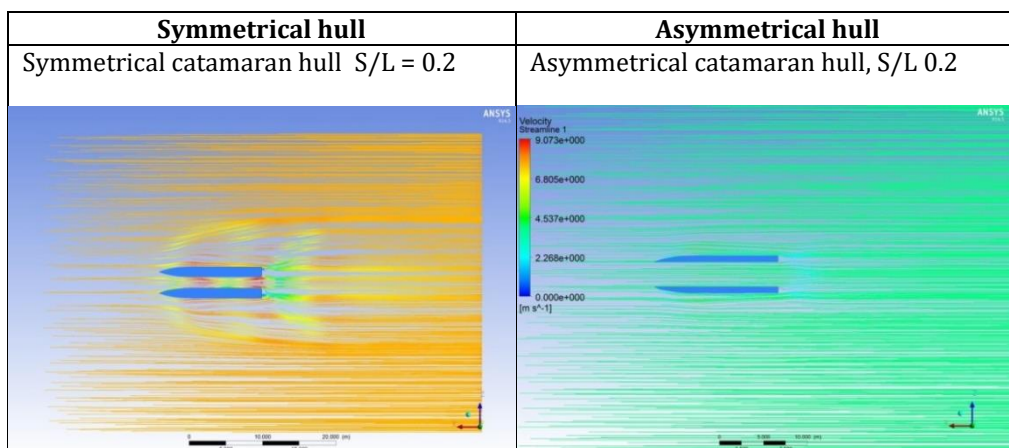
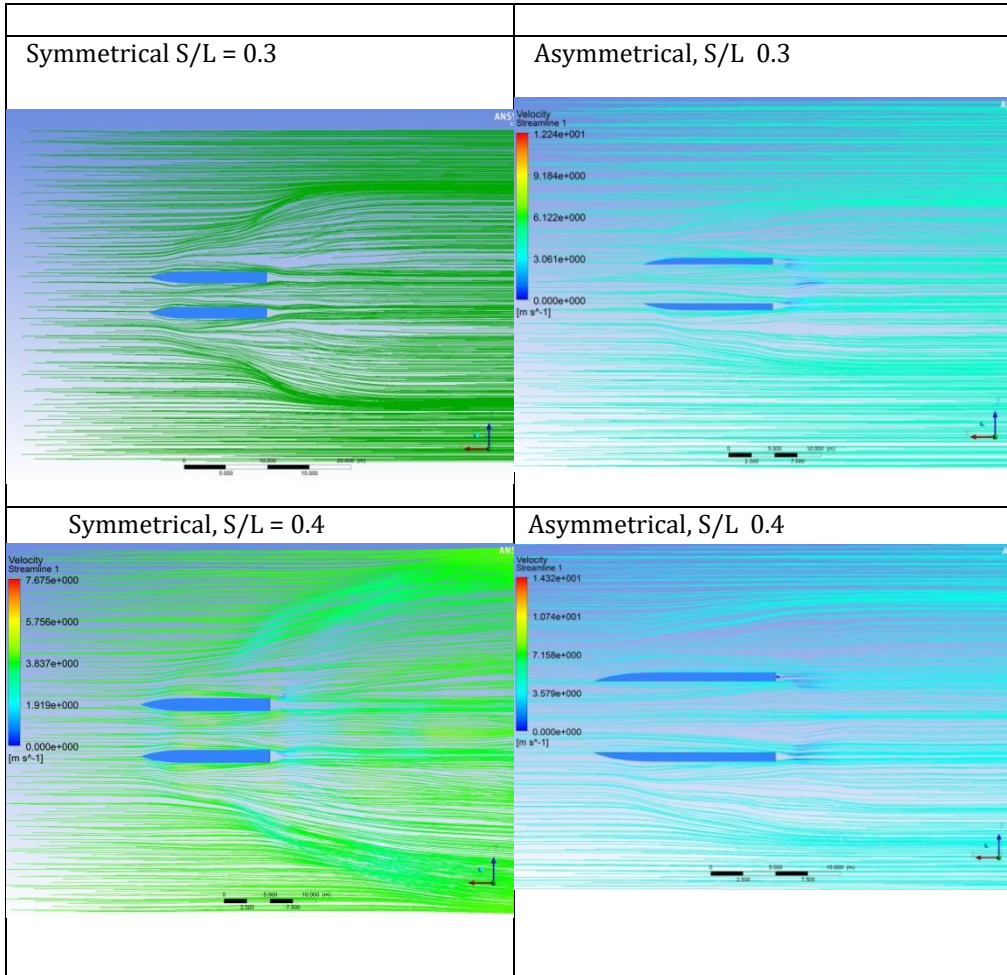


Figure 7. Symmetrical and asymmetrical hull graph with S/L 0.4

In Figure 7, at positions P5, P5' P9, and p9', symmetrical hulls experience a decrease in pressure compared to asymmetrical hulls with an S/L ratio distance of 0.4

Based on table 1 and 2, we can simulate in maxsurf that can be seen in figure 6.





4. Conclusion

Based on the simulation results, it can be concluded that the fluid flow around the hull is symmetrical and unsymmetrical due to the occurrence of flow interactions, and the pressure generated is relatively asymmetrical to the centerline. Furthermore, the distance between the S/L hulls influences changes in fluid flow patterns. The greater the distance between the hulls, the smaller the gastric pressure and elevation that occurs between the two hulls. The smaller the distance between the catamaran hulls (S/L), the greater the drag encountered, and the greater the transverse hull distance (S/L), the smaller the drag effect for each R/L ratio. The longitudinal gastric configuration (R/L) effect is more significant in symmetrical hulls than in asymmetrical hulls. This is because the drag coefficient for an asymmetrical hull is smaller than that of a symmetrical hull.

References

- [1] Moraes, H.B, Vascoellos, J.M and Almeida, P.M. (2007), Multiple Criteria Optimization Applied to High Speed Catamaran Preliminary Design, Ocean Engineering, Volume 34, pp. 133 – 147.
- [2] Seif, M.S.and Amini E. (2004), Performance Comparison Between Planing Monohull and Catamaran at High Froude Numbers , Iranian Journal of Science & Technology, Transaction B, Vol 28/ No. B4
- [3] Doctors, L.J. and Scrace, R.J. (2003). “Optimisation of Trimaran Sidehull For Minimum Resistance“, Proceedings of Seventh International Conference at Fast Sea Transportation, FAST‘2003, Ischia-Italy, Oktober
- [4] Insel, M and Molland, A F (1991). *An Investigation into the Resistance Components of High Speed Displacement Catamarans*. Meeting of the Royal Institution of Naval architects.
- [5] Molland, A.F and Utama I K A P., (2002) “Experimental and Numerical Investigations into the Drag Characteristics of a Pair of Ellipsoids in Close Proximity“, Proceedings of the Institution Of Mechanical Engineers: Engineering For The Maritime Environment, Vol 216 No. M2
- [6] Fundamentals of Fluid Mechanics 8th edition by Munson, Young and Okiishi
- [7] Gunawan, J., W. Surono, Andi. 2015. Identification and Allocation of Risks in the Superblock Project in Surabaya. Journal of Civil Engineering Primary Dimensions, Vol.4, No.2.
- [8] Haseeb, L., D. Bibi, and Rabbani. 2011. Problems of Projects and Effects of Delays in the Construction Industry of Pakistan. Australian Journal of Business and Management Research, Vol.1, No.5, p.41-50.
- [9] Kerzner, H. 1995. Project Management, System Approach to Planning, Scheduling, and Controlling. Fifth Edition. Van Nostrand Reinhold, New York.
- [10] Koontz, H. and C. O'Donel. 1994. Management. Erlangga, Jakarta.